RL-TR-97-248
Final Technical Report
March 1998

ANALYSIS OF OPTICALLY ACTIVE MATERIAL FIBERS

Syracuse University

Philipp Kornreich

APPROVED FOR PUBLIC RELEASE; DISTRIBUTION UNLIMITED.

AIR FORCE RESEARCH LABORATORY
ROME RESEARCH SITE
ROME, NEW YORK

This report has been reviewed by the Air Force Research Laboratory, Information Directorate, Public Affairs Office (IFOIPA) and is releasable to the National Technical Information Service (NTIS). At NTIS it will be releasable to the general public, including foreign nations.

RL-TR-97-248 has been reviewed and is approved for publication.

APPROVED: David Gruzya

DAVID J. GRUCZA
Project Engineer

FOR THE DIRECTOR: Gary D. Barmore

GARY D. BARMORE, Maj, USAF
Chief, Rome Operations Office
Sensors Directorate

If your address has changed or if you wish to be removed from the Air Force Research Laboratory mailing list, or if the addressee is no longer employed by your organization, please notify AFRL/SNDP, 25 Electronic Pky, Rome, NY 13441-4515. This will assist us in maintaining a current mailing list.

Do not return copies of this report unless contractual obligations or notices on a specific document require that it be returned.

REPORT DOCUMENTATION PAGE			Form Approved OMB No. 0704-0188

1. AGENCY USE ONLY *(Leave blank)*	2. REPORT DATE	3. REPORT TYPE AND DATES COVERED
	March 1998	Final Jun 96 - Jun 97

4. TITLE AND SUBTITLE

ANALYSIS OF OPTICALLY ACTIVE MATERIAL FIBERS

5. FUNDING NUMBERS

C - F30602-96-C-0172
PE - 62702F
PR - 4600
TA - P5
WU - PQ

6. AUTHOR(S)

Philipp Kornreich

7. PERFORMING ORGANIZATION NAME(S) AND ADDRESS(ES)

Syracuse University
Office of Sponsored Programs
113 Bowne Hall
Syracuse NY 13244-1200

8. PERFORMING ORGANIZATION REPORT NUMBER

N/A

9. SPONSORING/MONITORING AGENCY NAME(S) AND ADDRESS(ES)

Air Force Research Laboratory/SNDP
25 Electronic Pky
Rome NY 13441-4515

10. SPONSORING/MONITORING AGENCY REPORT NUMBER

RL-TR-97-248

11. SUPPLEMENTARY NOTES

Air Force Research Laboratory Project Engineer: David J. Grucza/SNDP/(315) 330-2105

12a. DISTRIBUTION AVAILABILITY STATEMENT

Approved for public release; distribution unlimited

12b. DISTRIBUTION CODE

13. ABSTRACT *(Maximum 200 words)*

This report describes a method of producing, and test results of, optical fibers having an optically active material at the core/cladding boundary. Two fibers were made and tested. The first has a thin AlCu alloy strip running the length of the fiber, the width of the strip covering approximately fifteen degrees of arc as seen looking at the fiber's cross section. The second has a thin CdTe semiconductor layer covering the fiber core. Both the AlCu strip fiber has absorption resonances in the transmission spectrum at 449 nm, 935 nm and 1140 nm, and exhibits both a polarization sensitive absorption at 1140 nm and birefringence at 1320 nm. The CdTe fiber exhibits a step in the transmission spectrum at a wavelength of 630 nm. This step is shifted towards shorter wavelengths from its value of 827 nm in the bulk material of the fiber preform.

14. SUBJECT TERMS

Optical Fiber, Thin Semiconductor Films, Active Optical Fiber

15. NUMBER OF PAGES

32

16. PRICE CODE

17. SECURITY CLASSIFICATION OF REPORT	18. SECURITY CLASSIFICATION OF THIS PAGE	19. SECURITY CLASSIFICATION OF ABSTRACT	20. LIMITATION OF ABSTRACT
UNCLASSIFIED	UNCLASSIFIED	UNCLASSIFIED	UL

ABSTRACT

We have analyzed both fibers having a thin AlCu alloy layer strip that covers about 15 degrees of arc at the core cladding boundary and fibers having a thin CdTe semiconductor layer cylinder at the core cladding boundary of the fiber. Both the AlCu alloy strip and the CdTe cylinder are about 5 nm thick. The AlCu alloy strip fibers have absorption resonance at 449 nm, 935 nm, and 1140 nm in the transmission spectrum and exhibit both a polarization sensitive absorption at 1140 nm and birefringence at 1320 nm. The CdTe fibers exhibit a step at a wavelength of 630 nm in the transmission spectrum. This step is shifted towards shorter wavelengths from its value of 827 nm in the bulk material in the fiber preform.

TABLE OF CONTENTS

LIST OF FIGURES

1. INTRODUCTION

We have analyzed both fibers having a thin AlCu alloy layer strip that covers about 15 degrees of arc at the core cladding boundary and fibers having a thin CdTe semiconductor layer cylinder at the core cladding boundary of the fiber. Both the AlCu alloy strip and the CdTe cylinder are about 5 nm thick. The fibers were fabricated in the Syracuse University Fiber Fabrication Research Laboratory. We measured the transmission spectrum of the AlCu alloy strip fibers. These fibers exhibit absorption resonance at 449 nm, 935 nm, and 1140 nm. The absorption at 1240 nm is polarization dependent. Light polarized parallel and light polarized perpendicular to the strip is absorbed at a different rates. The fiber is nearly single mode at 1140 nm. The absorption at 935 nm is somewhat polarization dependent and the absorption at 449 nm is less polarization dependent since the fiber is multi mode at these wavelengths. The interaction of the light with the metal is only strong in single mode fiber. The AlCu alloy strip fibers exhibit birefringence at 1320 nm where the fibers do not absorb light. All measurements were performed at room temperature.

We measured the transmission spectrum of the CdTe semiconductor cylinder fibers. The CdTe fiber preforms exhibit a step at a wavelength of 827 nm while the fibers drawn from this preform exhibit a step at a wavelengths at 630 nm in the transmission spectrum. The preforms absorb light with wavelength shorter than 827 nm and transmit light with wavelengths longer than 827 nm while the fibers drawn from this preform absorb light with wavelengths shorter than 630 nm and transmit light with wavelengths longer than 630 nm. Due to the quantum size effect this step is shifted substantially towards shorter wavelengths from its value of 827 nm in the bulk material. The step in the absorption spectrum of the preform at 827 nm is in agreement with its value in bulk crystalline CdTe. The step in the absorption spectrum of the preform is relatively sharp having a width of only 1.7 kT. Again, all measurements were performed at room temperature.

2. AlCu ALLOY STRIP FIBER

2a AlCu Alloy Fiber Fabrication

We have fabricated AlCu alloy fiber. The main requirement is that during the fiber pulling process the plasto-viscosity of the glass is somewhat larger than the plasto-viscosity of the Optically Active Material, the AlCu alloy film. This has to be true throughout the preform

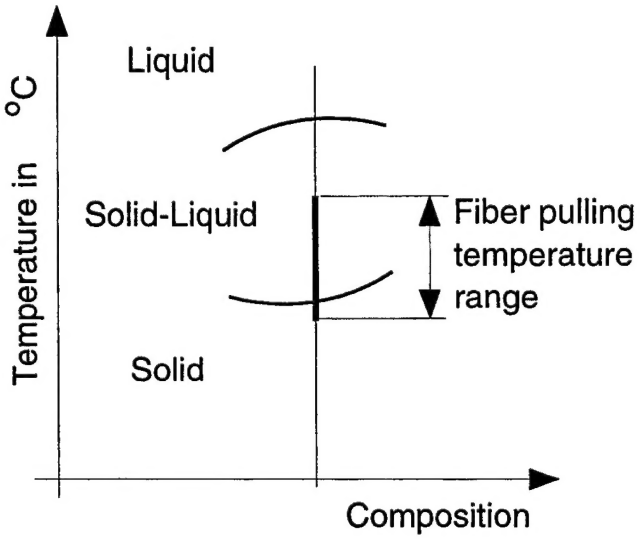

Fig. 1. Typical phase diagram of composite materials. It would be best to perform the fiber pulling process at temperatures where the liquid and solid phases of the optically active material coexist.

taper in the fiber pulling burner. This is accomplished by choosing the appropriate glasses and Optically Active Materials as well as by adjusting the temperature profile of the fiber pulling burner and the force applied to the fiber. In order to assure that the AlCu alloy, in this case, has a plasto-viscosity less than the glass during the fiber pulling process it has to have a region in the phase diagram at the fiber pulling temperatures where the liquid and solid phases of the AlCu alloy coexist liquid as shown in Fig. 1.

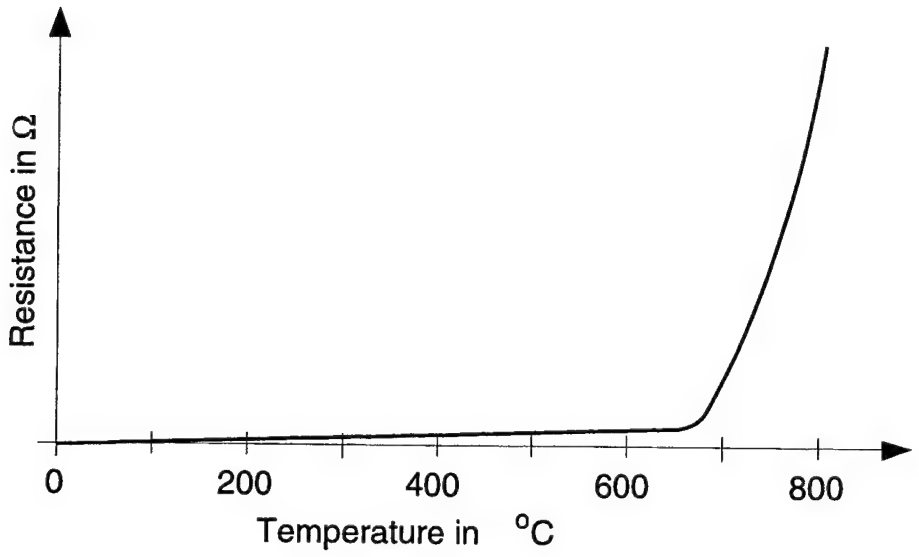

Fig. 2. A plot of the resistance of a vacuum deposited AlCu alloy film using an 65% Cu 35% Al alloy as the source material. The film was deposited on a Vicor tube and protected by a SiO_x coating.

For example, the metal used in Metal Strip fibers has to have a plasto-viscosity less than the type 7052 type glass. We have empirically determined that the metal has to have a melting point less than 700 °C. In order to determine the melting points of the AlCu alloy films we vacuum deposited the films on Vicor tubes and measured the resistance of the films while heating the Vicor tubes. The resistance increases greatly when the films melt. We vacuum deposited films using an 65% Cu 35% Al alloy as the source on Vicor tubes. These films except for the ends where covered with vacuum deposited SiO_x. These coated Vicor tubes were heated and the resistance of the AlCu alloy film was monitored. The resistance as a function of temperature are shown in Fig. 2. We observe that the resistance increases gradually until a temperature of about 680 °C is reached. At 680 °C, where the alloy melts, the resistance increases rapidly as shown in Fig. 2. We observe that these films exhibit a melting point of 680 °C. We deposited this alloy on three different Vicor tubes and

measured the resistance as function of temperature. We obtained identical results.

Using this process we have fabricated near single mode AlCu strip fibers. We examined about 25 cross sections of this fiber with our Vickers fiber microscope and found it to be exceedingly uniform. The absorption region surrounding the metal strip is clearly visible.

2b AlCu Alloy Fiber Measurements

We measured the transmission spectrum of the AlCu alloy strip fibers at room temperature using an unpolarized white light source. The data is shown in Fig. 3. Fiber samples about 30 cm long were used. Note the resonances at 449 nm, 935 nm, and 1140 nm. These resonances correspond to optical frequencies of 6.677×10^{14} Hz, of 3.206×10^{14} Hz, and of 2.630×10^{14} Hz respectively. These frequencies are much too low to be plasma resonance frequencies. Plasma resonances are of the order of 10^{16} Hz. Perhaps, the resonances that we observe correspond, approximately, to etalon resonances in the approximately 5 nm thick metal film. We assume that the fundamental mode, where the metal film thickness of 5 nm corresponds to one half wavelength occurs at a wavelength of 935 nm. Thus the wavelength in the metal is 10 nm at this frequency. The wavelength in the metal is equal to the wavelength in vacuum, 1140 nm, divided by the index of refraction n in the metal at this wavelength. This gives an index of refraction $n_o = 93.5$ at a light frequency f_o of 3.206×10^{14} Hz. We assume that the resonance at 449 nm is the next higher mode where the metal thickness corresponds to a complete wavelength. This yields an index of refraction n_1 of 89.8 at a light frequency of 6.677×10^{14} Hz.

The index of refraction squared n^2 at a light frequency f and a plasma frequency f_p is given by:

$$n^2 = 1 + \frac{f_p^2}{f^2} \qquad (1)$$

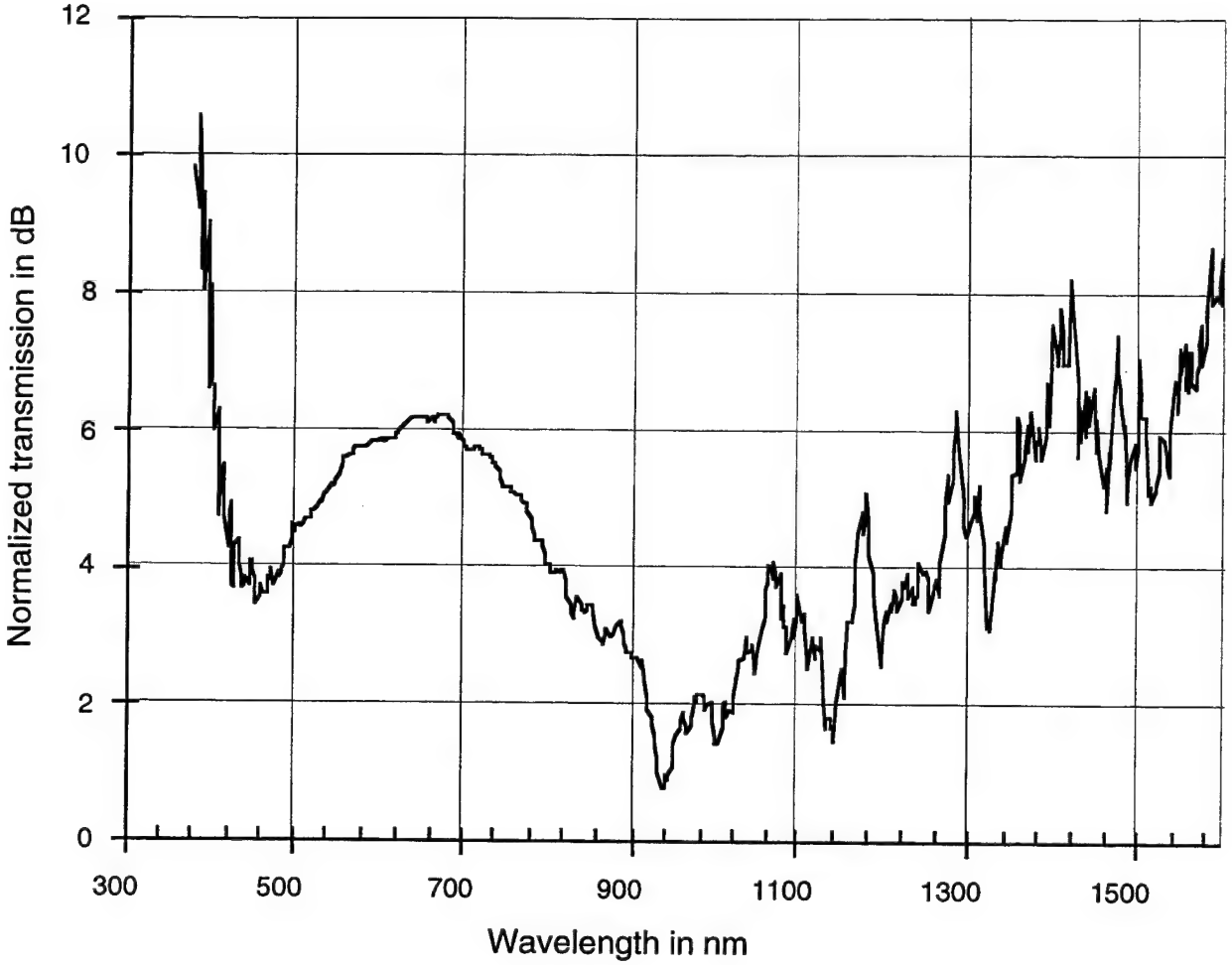

Fig. 3. The transmission spectrum of the AlCu alloy strip fibers. Note the absorption resonances at 449 nm, 935, nm and 1140 nm. Fiber samples about 30 cm long were used.

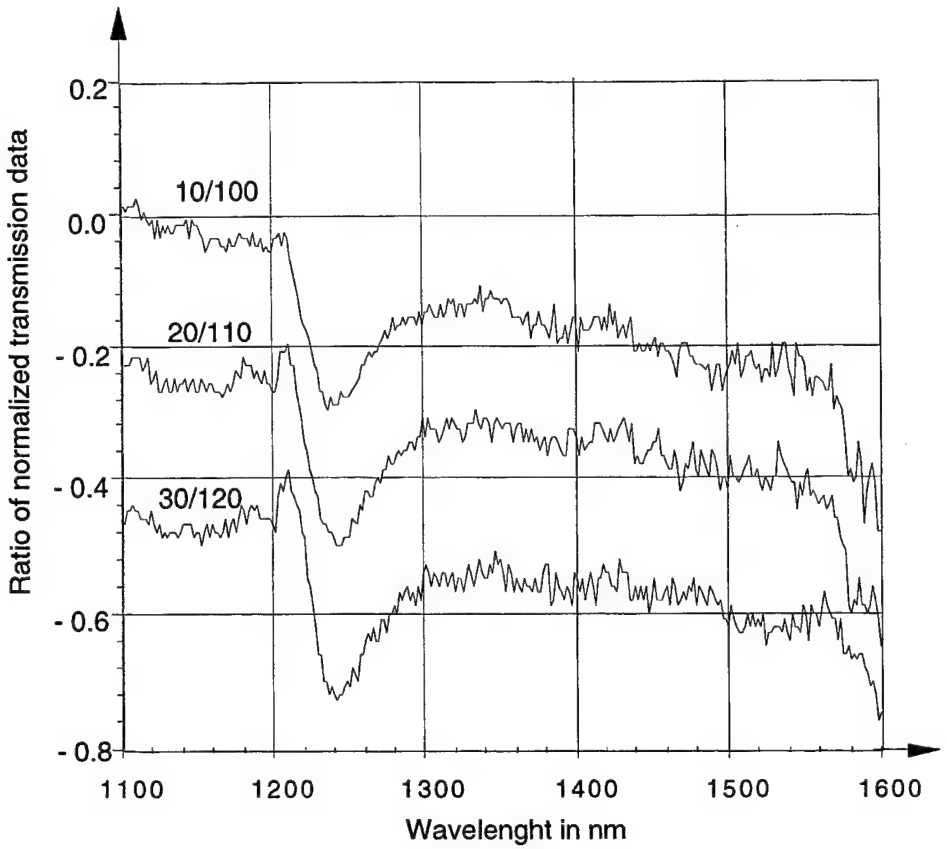

Fig. 4. The ratio of the transmission spectrum of the AlCu alloy strip fibers with polarizations that differ by 90 degrees. The first curve is the ratio of the transmission spectrum at a polarization of 10 ° to the transmission spectrum at 100°. The second curve is the ratio of the transmission spectrum at a polarization of 20 ° to the transmission spectrum at 110°, and the third curve is the ratio of the transmission spectrum at a polarization of 30 ° to the transmission spectrum at 120°.

This equation yields a plasma frequency f_p of 2.998 x 10^{16} Hz for the fundamental mode with a wavelength of 935 nm. This plasma frequency has the right order of magnitude. The plasma frequency f_{p1} of the next higher mode with a resonance at 449 nm is 5.995 x 10^{16} Hz. Note that the plasma frequency of the second mode is twice as large as the plasma frequency of the fundamental mode. The plasma resonances also have

modes due to the confinement of the electrons in the thin metal film. It appears that the plasma resonance modes interact only with light electromagnetic modes that have the same spatial symmetry.

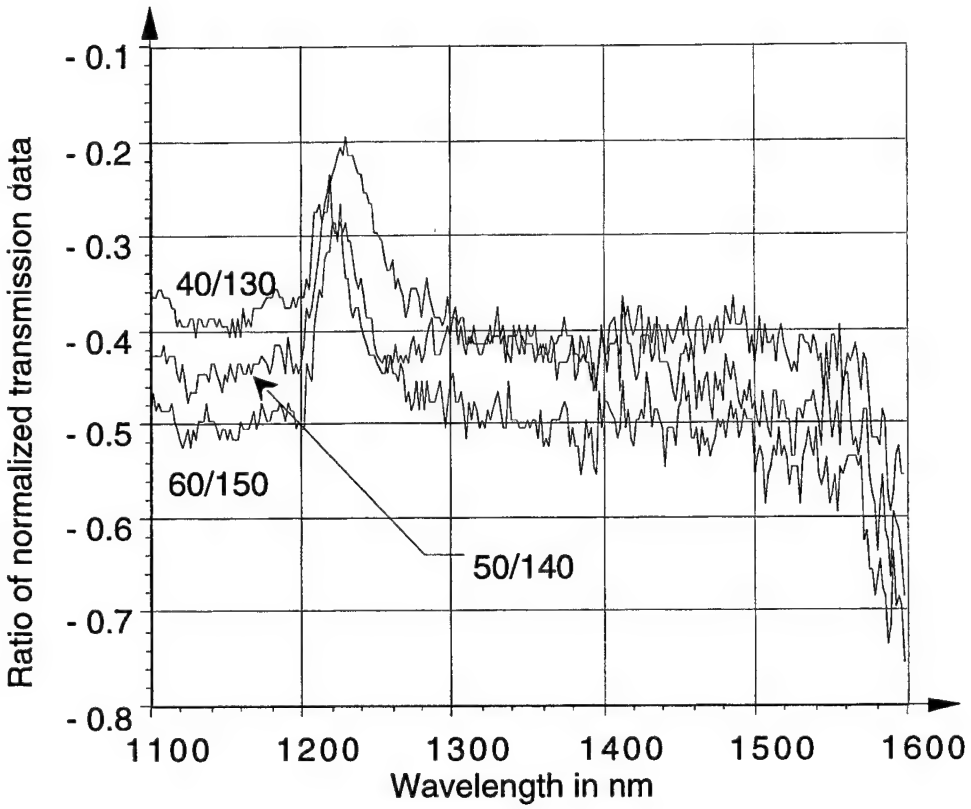

Fig. 5. The ratio of the transmission spectrum of the AlCu alloy strip fibers with polarizations that differ by 90 degrees. The first curve is the ratio of the transmission spectrum at a polarization of 40 ° to the transmission spectrum at 130°. The second curve is the ratio of the transmission spectrum at a polarization of 50 ° to the transmission spectrum at 140°, and the third curve is the ratio of the transmission spectrum at a polarization of 60 ° to the transmission spectrum at 150°.

The metal strip fiber should absorb light polarized parallel to the metal strip and light polarized perpendicular to the metal stripe differently. In order to illustrate the polarization properties of the metal

strip fibers we divided the transmission spectrum taken at polarizations that differ by 90° and plotted the results.. This is shown in Fig. 4, 5, and 6.

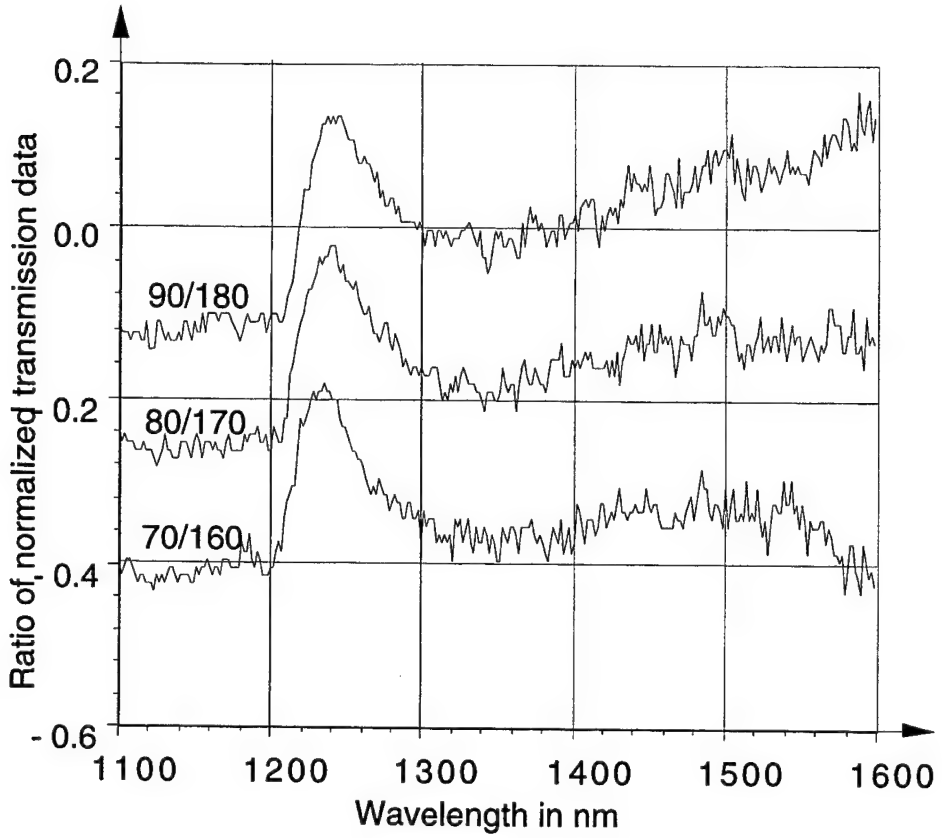

Fig. 6. The ratio of the transmission spectrum of the AlCu alloy strip fibers with polarizations that differ by 90 degrees. The first curve is the ratio of the transmission spectrum at a polarization of 70 ° to the transmission spectrum at 160°. The second curve is the ratio of the transmission spectrum at a polarization of 80 ° to the transmission spectrum at 170°, and the third curve is the ratio of the transmission spectrum at a polarization of 90 ° to the transmission spectrum at 180°.

The metal strip fibers have yet another application. They can be used as very high dispersion fibers for "True Time Delay" optical processors for Phased Array Antenna applications. Near the resonances exceedingly high dispersions can be achieved in relatively short pieces of fiber of about 15

cm. A light Frequency Dependent Delay can be generated by using a fiber where the light propagating through it has a phase $\phi(\omega)$ that depends on the square of the frequency for some frequency range:

$$\phi(\omega) = \phi(\omega_p) + b(\omega - \omega_p)^2 + \ldots \qquad (2)$$

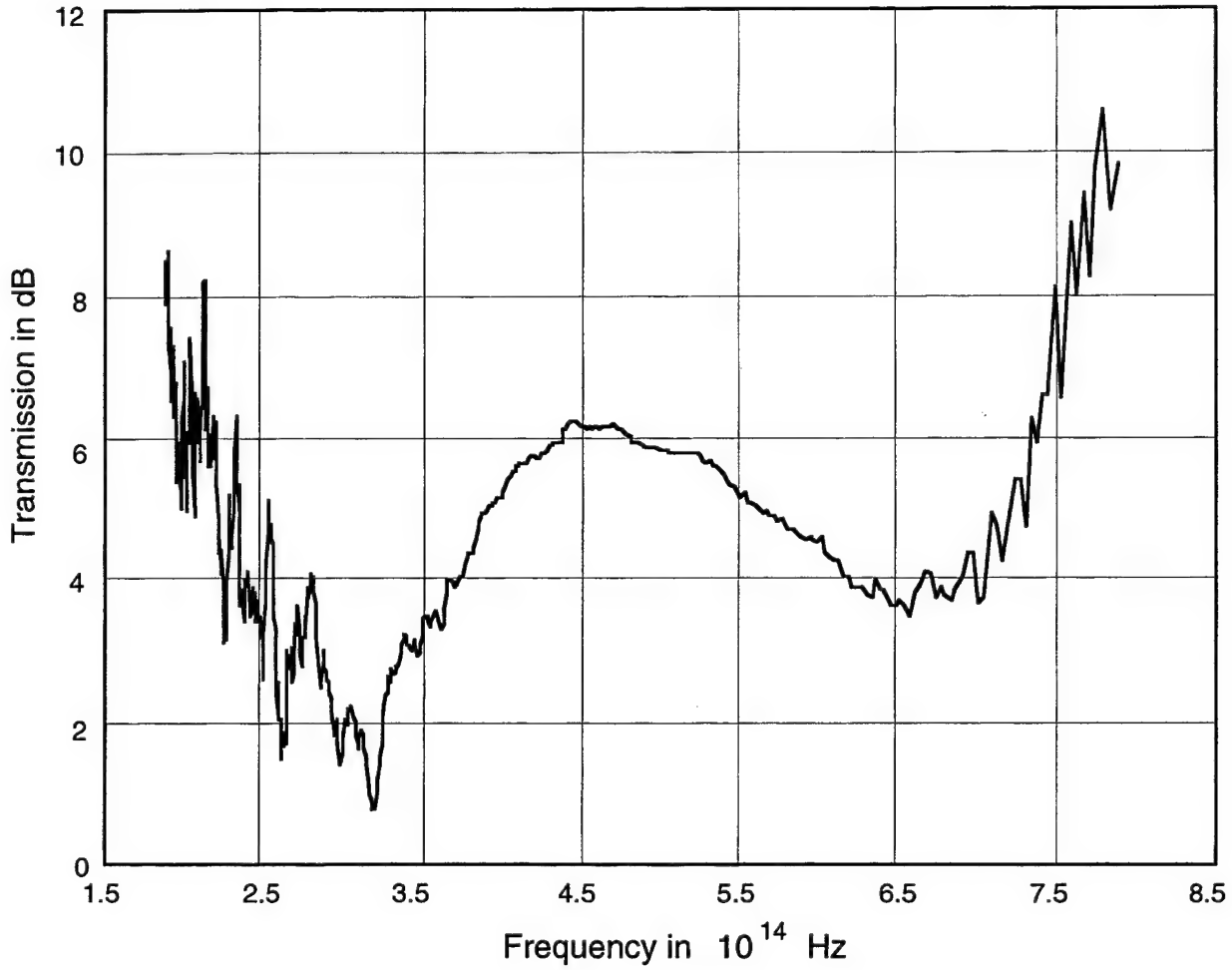

Fig. 7. The logarithmic transmission spectrum of the AlCu alloy strip fibers as a function of the radial frequency w of the light.

where ω_p is the frequency about which the Taylor series expansion is performed. Consider the case where the angular frequency ω consisting of

the sum two frequencies, ω_o and ω_{RF}. Here ω_o is the frequency of the light and ω_{RF} is a "Radio Frequency" at which, say, a phased array antenna would operate. The light, in this case, has a single side band modulation as is conventional in "True Time Delay" heterodyne optical phased array antenna processors. By substituting into equation 1 we obtain:

$$\phi(\omega) = \phi(\omega_p) + b(\omega_o - \omega_p)^2 + 2b\omega_{RF}(\omega_o - \omega_p) + b\omega_{RF}^2 + \ldots \qquad (3)$$

The last term can be neglected since the "radio Frequency" is many order of magnitude smaller than the light frequency. Indeed, there is a phase term $2b\omega_{RF}(\omega_o - \omega_P)$ that depends both on the radio frequency and the light frequency. The linear radio frequency dependence is necessary for a true time delay. This phase delay can be changed by varying the optical frequency ω_o with a variable wavelength laser. In Fig. 7 we replotted the logarithm of the spectral response as a function of light frequency. The phase $\phi(\omega)$ can be calculated from the logarithm of the spectral response by the use of the Hilbert transform. Values for the expansion coefficient b for light frequency where the first derivative of the phase $\phi(\omega)$ with respect to the light frequency ω_o is equal to zero can be obtained from Fig. 7. We obtain for b a values of the order of 10^{-24} radians-seconds^2 per meter (1000 radians-psec.^{2} per km).

3 SEMICONDUCTOR CYLINDER FIBERS

3a Semiconductor Cylinder Fiber Fabrication

At present the semiconductor layers are deposited in a closed evacuated ampoule as shown in Fig. 4.1. The ampoule is constructed by closing one end of a cleaned 3 mm outside diameter and 1.8 mm inside diameter glass tube. A small amount of about 25 mg of semiconductor powder is loaded into one tube and pushed to the closed end with a rod. Next, a 1 mm diameter core rod is placed into the tube as shown in Fig. 8. This process is similar to loading a flint lock gun. To load a flint lock gun

an amount of powder is placed into the barrel of the gun and pushed to the far end with a ram rod. Next a ball is placed in to the barrel. A soft

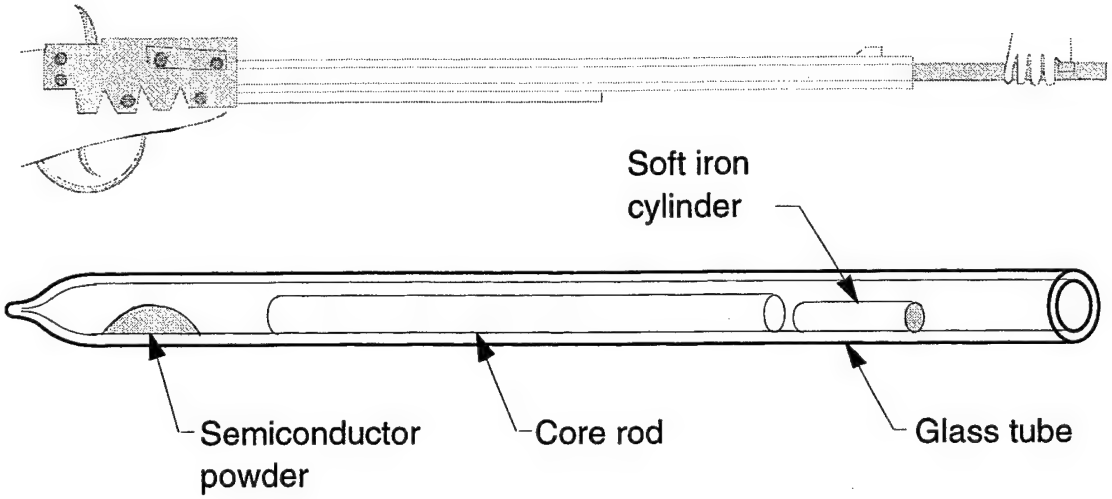

Fig. 8. Glass tube that has been closed at one and containing some semiconductor powder and a core rod. The process of loading of the semiconductor powder and core rod is similar to the process of loading an old flint lock gun.

iron cylinder is placed in front of the core rod. The soft iron cylinder is held in place by an external magnet during the initial phase of the evaporation so that the core rod will not be sucked into the vacuum system. If need be this iron cylinder can be used to move the core rod in the evacuated tube for multi layer semiconductor deposition.

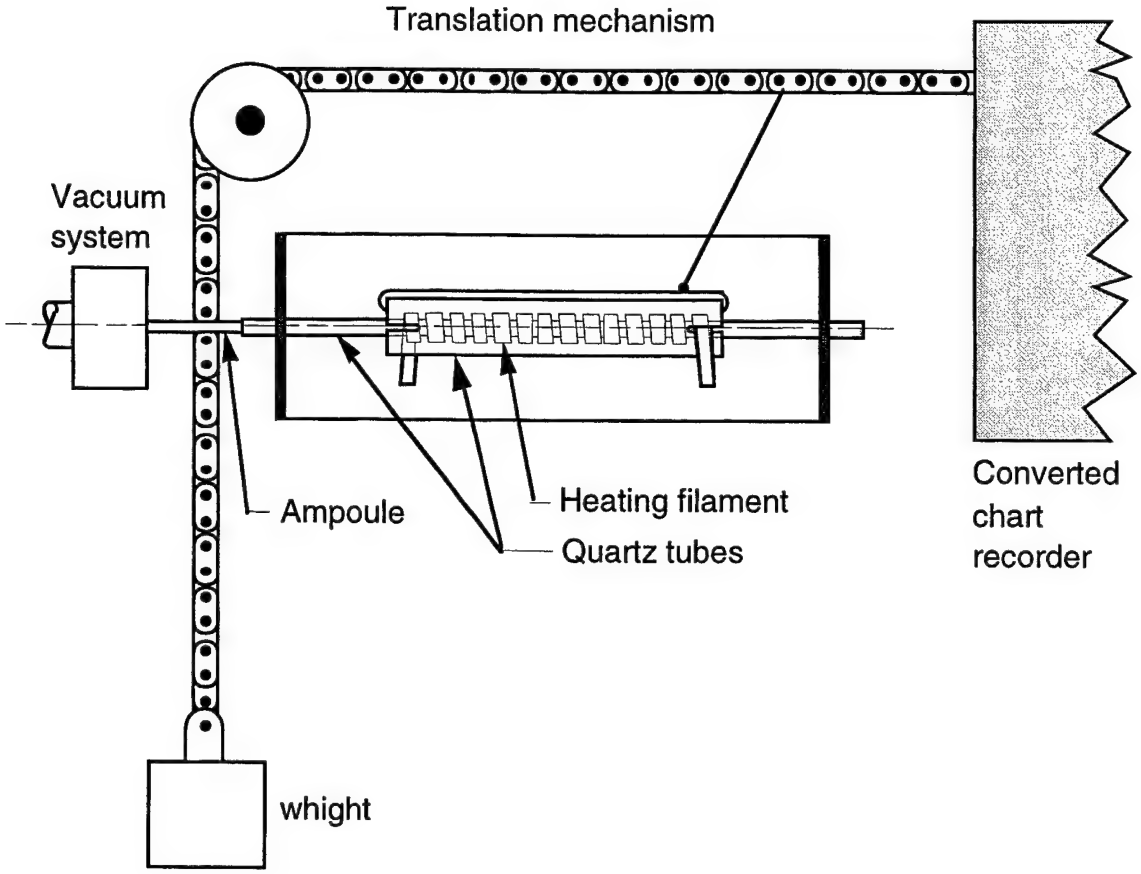

Fig. 9. The ampoule is placed into a traveling heater with its open end connected to a vacuum system. The semiconductor powder is located in the region of the heater filament. The semiconductor is deposited on the core rod and the inside of the ampoule tube where the ampoule emerges from the heater.

The ampoule is placed into a traveling heater as shown in Fig. 9. The open end of the ampoule is connected to a small vacuum system capable of producing a 10^{-7} Torr vacuum. The ampoule is heated to a temperature sufficiently high to evaporate the semiconductor but not hot enough to collapse the ampoule tube. The semiconductor is deposited on the core rod and the inside of the ampoule tube where the ampoule emerges from the heater see Fig. 8. After completing the deposition of the semiconductor layer, the ampoule is sealed at the end near the vacuum system.

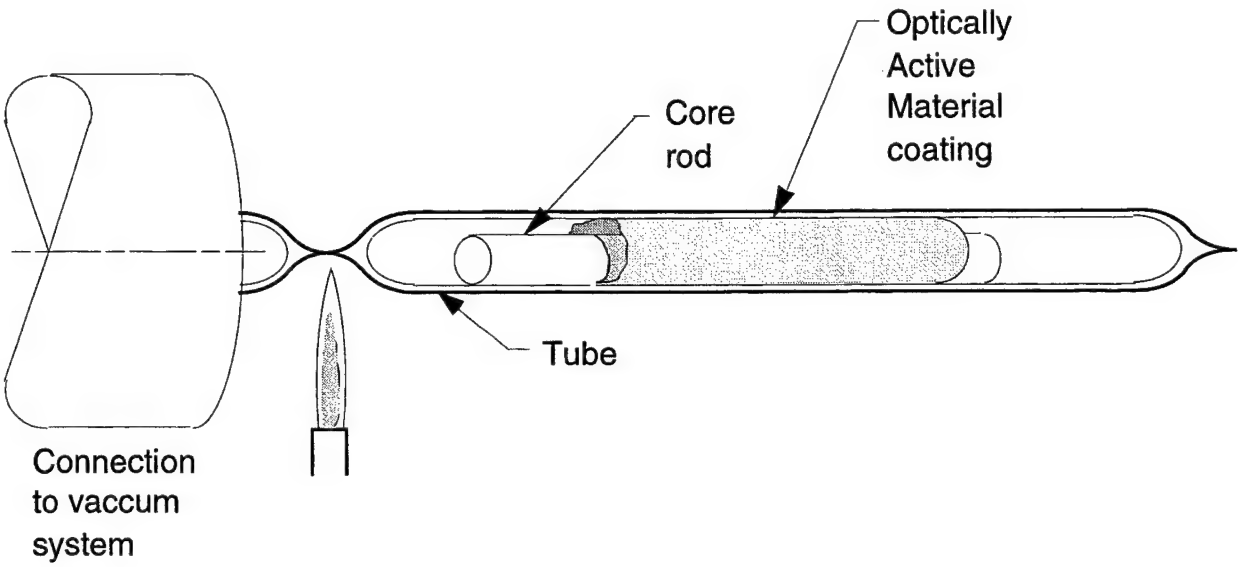

Fig. 10. The ampoule is pinched off near the vacuum pump end after the core rod and the inside of the ampoule tube are coated with the semiconductor.

We have tested a method that uses light to evaporate the semiconductor without heating the ampoule glass. This would allow us to evaporate high temperature semiconductors. This method uses the fact that light is absorbed by a semiconductor while the glass is transparent to the light. We, first, used an Argon laser operating with an output of 2.25 W to evaporate CdTe semiconductor in a sealed evacuated ampoule. We, next, spread out the laser beam using a cylindrical lens with a focal length of 38.2 mm and placed the ampoule about 300 mm from the lens. The lens spreads out the laser beam to about 15 mm at the location of the ampoule. The ampoule was placed on a motorized translation stage that moved at 25.4 mm (1 inch) per hour. The Argon laser was set to 4.5 W. The end of the ampoule where the semiconductor was located and the adjoining region of the ampoule where covered by the spread out laser beam. The translation stage moved the semiconductor pile, gradually, across the spread out laser beam. Thus, as the ampoule moves, less and less of it is covered by the laser beam. This is similar to the arrangement with the traveling heater described above. We expected the deposition to occur

where the ampoule emerges from the laser beam. However, we observed that the deposition occurred in the region illuminated by the laser in the first few minutes. We tried two ampoules. The deposition in one ampoule was 13 mm long and the other was about 15 mm long.

We plan to use a mirror that forms an elliptical cylinder with a gas discharge tube in one focal line and the ampoule in the other focal line. The lamp and mirror would move along the ampoule at the same rate as the present heater coil. One would require a gas discharge tube having about 350 W concentrated in the spectral range between 400 and 550 nm.

Without the semiconductor present to produce a high gas pressure inside the ampoule, the ampoule can be collapsed. The ampoule is

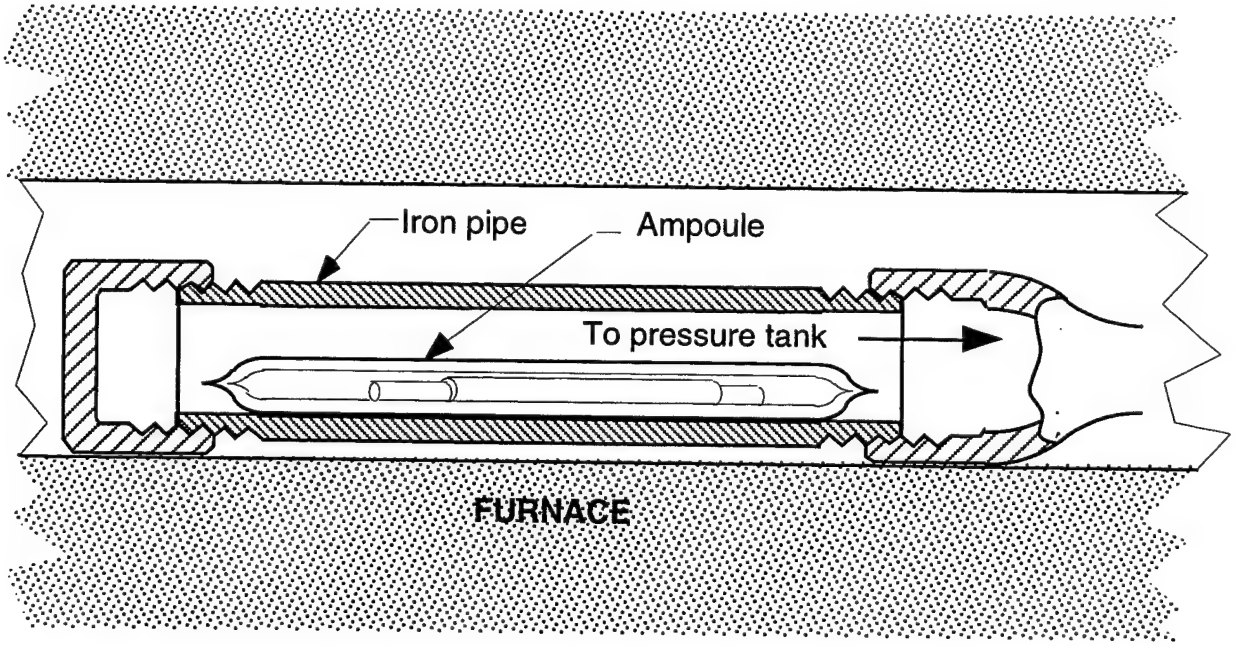

Fig. 11. The ampoule consisting of the first cladding tube that has been evacuated and closed on both ends and contains the coated core rod is collapsed in a pressurized iron tube located in a furnace.

collapsed in a pressurized iron tube as shown in Fig. 11, located in a furnace. We have used pressures up to 85 lb per ft^2 or 5.784 Atm. and temperatures

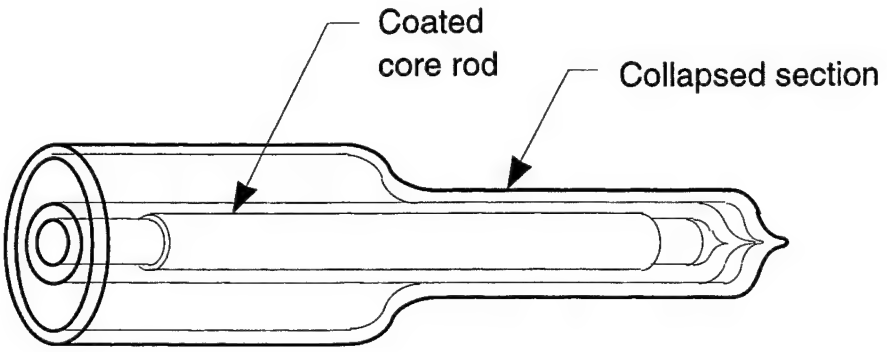

Fig. 12. After collapsing the first tube onto the coated core rod other tubes are collapsed onto the collapsed first tube.

of 650° C.

The other tubes are collapsed using only atmospheric pressure in the furnace shown in Fig. 13. The tubes closed at one end and are evacuated with the vacuum pump shown in Fig. 13. The tubes are collapsed sequentially onto the collapsed ampoule. Both the previously collapsed structure and the tube to be collapsed next are thoroughly cleaned. The preform is stationary while the furnace can be moved to uniformly collapse the tubes. A mechanical vacuum pump capable of a vacuum of 10^{-3} Torr is located near one end of the furnace.

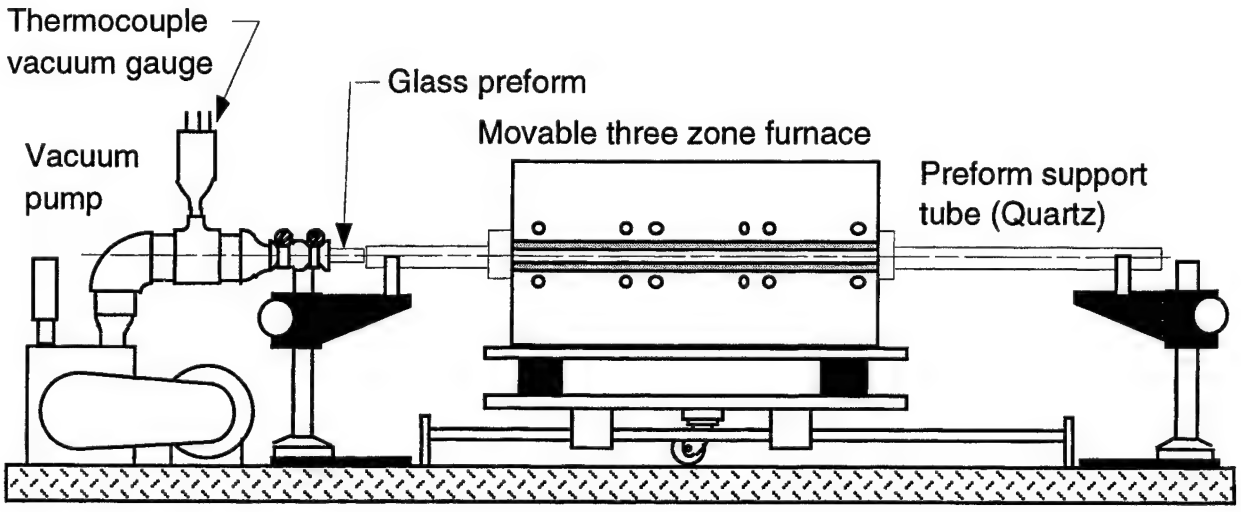

Fig. 13. Furnace for collapsing Pyrex type glass.

We have arranged the temperature profile in a three zone furnace to have a gradient of about 20 °C. The furnace is hottest near the end facing away from the vacuum pump. The glass tube to be collapsed is located inside a quartz support tube. The glass tube to be collapsed is attached to the vacuum pump The furnace can be moved on linear bearings to insert the tube into the furnace. The heating elements of each of the three zones of the furnace are connected to a variable autotransformer or "Variac". The three Variacs have a common shaft so that the temperature in the furnace can be changed with a single control. The three Variacs are off set on the common shaft to generate a temperature gradient of about 20 °C in the furnace. A temperature profile of the furnace when used for collapsing

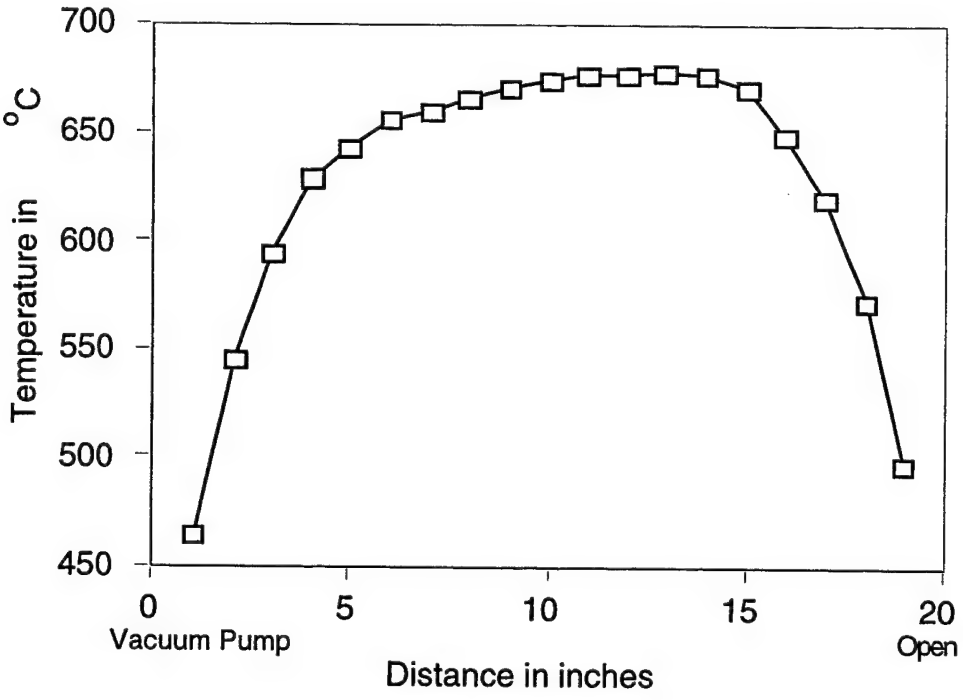

Fig. 14. Temperature profile of furnace for preform collapsing type 7740 Pyrex glass tubes..

type 7440 Pyrex tubes is shown in Fig. 14. Note the slope of the temperature profile in the "active" region of the furnace. This temperature profile results in the glass tubes collapsing first at its farthest end from

the vacuum pump where the furnace is hottest. The collapsing process than propagates towards the vacuum pump.

At present we have 1 mm diameter type 7720 glass rods having an index of refraction of 1.487 and four type 7052 glass tubes having an index of refraction of 1.484 on order.

An experiment was carried out to see at what temperature one of the above glass tubes would sag under its own weight. The tube become strongly elliptical at 654 °C.

One can obtain an approximate expression for the time $t_{collapse}$ in minutes required to collapse the tube:

$$t_{collaps} = \beta_o \frac{w}{DP} \exp\left[- \frac{T}{T_o} \right] \qquad (4)$$

where , w is the wall thickness of the tube in mm, D is the outside diameter of the tube in mm, P is the pressure in Atmospheres, and T is the collapsing temperature in °C. Here β_o and T_o are constants depending on the plasto-viscosity of the glass. The larger the ratio of outside diameter D of the tube to its wall thickness w, the larger the pressure P, and the larger the temperature T the quicker the tube will collapse.

Since the 1 mm diameter type 7720 glass rods are expensive we use type 7740 Pyrex tubes for calibrating the fiber pulling process. We use the following type 7740 Pyrex material:

	I. D.	O. D.	Collapsed dia.	
Rod	1.0 mm			n = 1.4714
Tube*	1.8 mm	2.8 mm	2.366 mm	n = 1.4716
Tube	2.7 mm	4.2 mm	3.994 mm	n = 1.4716
Tube	5.6 mm	9.5 mm	8.651 mm	n = 1.4715

*This is the ampoule tube.

These tubes are collapsed sequentially to form the preform. The preform diameter D_{Calc} is predicted to be 8.651 mm. The measured preform had a diameter of D_{Meas} = 8.5 mm and index of refraction of 1.4724.

Fiber has been drawn from the above described preforms. A particular portion of the a fiber was measured with the fiber microscope. It had an outside diameter of 93 μm and it exhibited a core of about 11 μm diameter.

Unfortunately, both the core and cladding of a fiber pulled from such a preform has the same index of refraction. Thus, the core of this fiber will not guide light.

We also have 2.1 mm diameter type 3320 (Uranium) glass rods with both a nominal and measured index of refraction of 1.481. These glass rods appear somewhat yellow. They have an absorption peak at 706.7 nm and an absorption edge sloping from 490 to 518 nm. These fibers absorb light with wavelengths shorter than 490 nm. Fibers fabricated with these glass rods will guide light.

3b Properties of Semiconductor Cylinder Fibers

We have tested CdTe **S**emiconductor **C**ylinder **F**ibers (SCF) some three years ago at Rome Laboratory. Those fibers had a CdTe cylinder surounding a core with a diameter of 70 μm. Since the core and cladding had the same index of refraction the semiconductor cylinder provided the guiding. Even though the interaction between the light and the semiconductor in this multi mode fiber was very weak, we obtained the transmission spectrum of the fibers. The transmission spectrum of the fibers was similar to the transmission spectrum of bulk CdTe. The fiber pieces tested were about 8 mm long. This result demonstrated that at least CdTe survived the fiber fabricating process. This inspired us to initiate a research project to develop fibers with Optically Active Material layers at the core cladding boundary. The process of fabricating such fibers is now well understood. We have developed a process for fabricating fibers with Optically Active Material layers at the core cladding boundary.

We have recently tested a SCF with a CdTe semiconductor at the core cladding boundary. These fibers had a core diameter of 10 μm and a smooth uniform semiconductor layer. Since the core diameter is near single mode the interaction is much stronger. This time the transmission spectrum does exhibit a blue shift due to the quantum size effect of the very thin, approximately 5 nm thick, semiconductor layer.

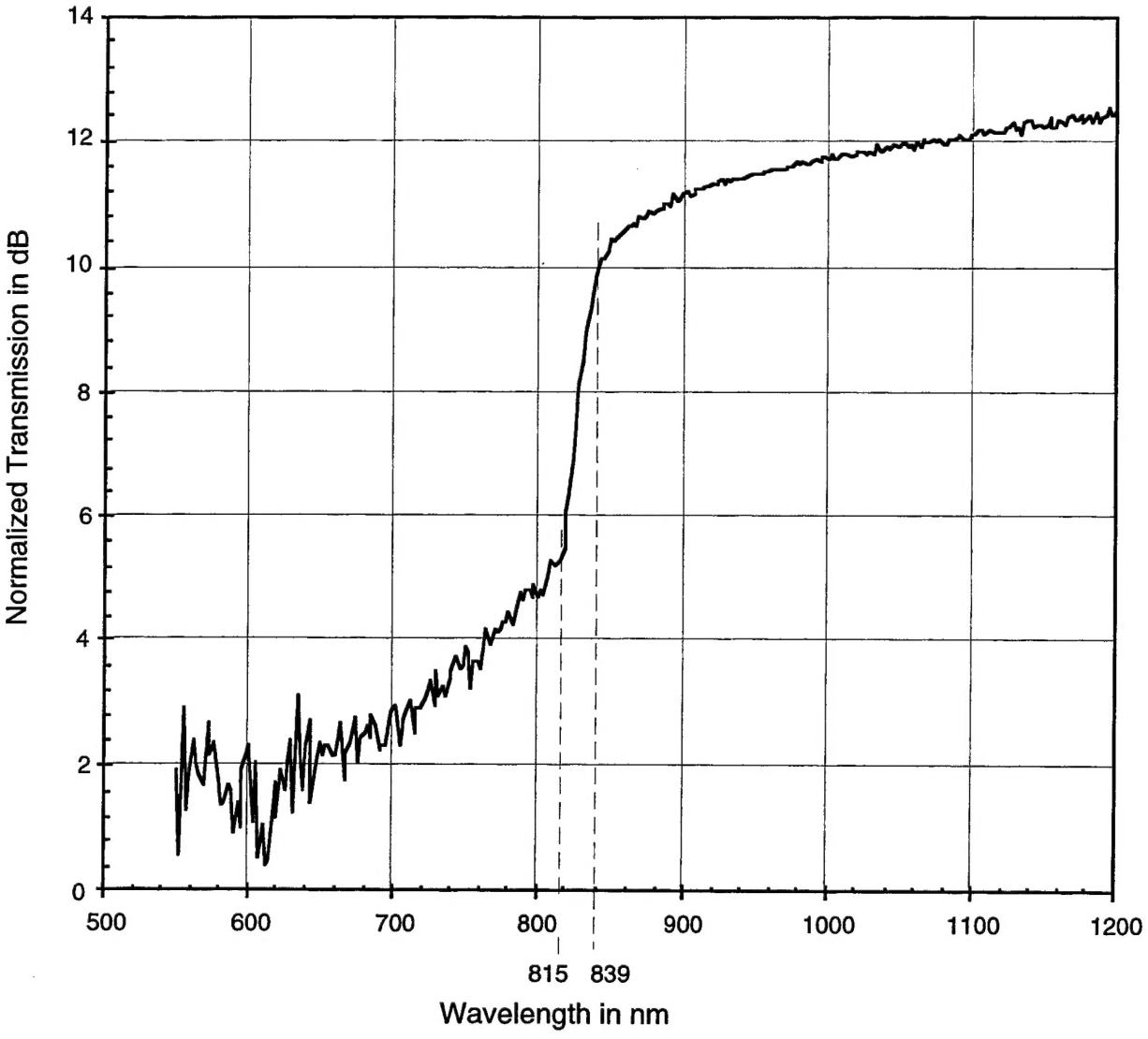

Fig. 15. The transmission spectrum of CdTe cylinder fiber preform.

We first measured the transmission spectrum of the fiber preform. The fiber preform exhibits a step at a wavelength of 827 nm in the transmission spectrum as shown in Fig. 15. This is in agreement with its value in bulk crystalline CdTe. The step is relatively sharp having a width of only 1.7 kT. A measurements were performed at room temperature.

We pulled a fiber from this preform. The fiber exhibits a step at 630 nm. That is the step is shifted, as expected, towards the blue in the spectrum by about 197 nm. This corresponds to a blue shift of 469 meV. The observation of a blue shift is encouraging since no such phenomenon was observed in the original CdTe Cylinder Fibers. The measurements were performed on 10 mm long pieces of fiber. It would be necessary to pump these fibers with light having a wavelength shorter than, say, 440 nm.

The theoretical shift in energy ΔE in eV due to a confinement of electrons with an electron effective mass ratio $m_e^* = 0.064$ and a holes with a hole effective mass ratio $m_h^* = 0.1$ in a semiconductor layer of thickness a is:

$$\Delta E = \frac{\hbar^2 \pi^2}{2 m_o e a^2} \left[\frac{1}{m_e^*} + \frac{1}{m_h^*} \right] \qquad (5)$$

Since we know the shift in energy $\Delta E = 0.469$ eV we can use equation 4 to calculate the thickness a of the semiconductor layer. We obtain a thickness a of 4.533 nm and a thickness of approximately 0.409 μm of the semiconductor film in the preform. This is in good agreement with the predicted values.